Guy T. Houlsby, Barry G. Clarke and C. Peter Wroth

ANALYSIS OF THE UNLOADING OF A PRESSUREMETER IN SAND

REFERENCE: Houlsby, G. T., Clarke, B. G. and Wroth, C. P., "Analysis of the Unloading of a Pressuremeter in Sand", The Pressuremeter and Its Marine Applications, ASTM STP 950, J.-L. Briaud and J. M. E. Audibert, Eds., American Society for Testing and Materials, 1986.

ABSTRACT: The self-boring pressuremeter offers a particular advantage in that it can be installed in the ground with minimal disturbance. The loading stage of a pressuremeter test in sand has been analysed previously in terms of the shear modulus, angle of friction, angle of dilation and the initial horizontal stress and pore pressure. A new analysis is presented of the unloading stage of the pressuremeter test; this can provide a separate check on the parameters measured during the loading stage. An optimisation routine is used to fit the properties to the results of a series of tests at a site in Wales. Various important effects are discussed, including the effect of stress level on the shear modulus and the relevant value of the angle of friction to be used for the unloading stage.

KEYWORDS: analysis, angle of dilation, angle of friction, case history, in situ stress, pressuremeter test, sand, shear modulus, unloading

INTRODUCTION

The self-boring pressuremeter is a site investigation device which is gaining wide acceptance as a means of determining accurately strength and deformation properties of soils. The test involves the installation of a cylindrical pressuremeter into the ground with minimal disturbance, and subsequent inflation of the pressuremeter membrane with measurement of the associated strain. Hughes, Wroth and Windle [1] presented an analysis of the loading of a pressuremeter in sand using a simplified model of material behaviour. In the model the sand is assumed to be isotropic linear elastic until yield occurs when the Mohr-

Prof. Wroth is Professor of Engineering Science at the Department of Engineering Science, Oxford University, Parks Road, Oxford OX1 3PJ, U.K. Dr. Houlsby is a University Lecturer in the same department. Dr. Clarke is a University Lecturer at the Department of Geotechnical Engineering, University of Newcastle upon Tyne, Newcastle NE1 7RU, U.K.

Coulomb condition is satisfied; the material then flows plastically at a fixed angle of dilation. The analysis represents a refinement of the analysis presented by Gibson and Anderson [2]. From this analysis the shear modulus, angle of friction and angle of dilation can be determined.

During a typical pressuremeter test one or two unload-reload cycles are carried out, and at the end of the test, data may also be obtained from the final unloading. These data contain valuable information about the soil properties, which may be used for comparison with the results obtained from the loading section. There are certain advantages in making use of these data in that they are less sensitive to any initial disturbance caused by the installation of the pressuremeter. This paper is concerned with an analysis of the unloading section of the test, using the same model as that used by Hughes, Wroth and Windle [1]. The key feature of the new analysis is that it accounts for the fact that the unloading takes place from an initially non-homogeneous stress state which has been set up by the preceding expansion phase. The results of the analysis are compared with a set of high quality pressuremeter test results in sand.

The importance of the new analysis lies in the fact that the loading analysis usually requires some knowledge of the value of ϕ_{cv} for the sand. If independent information can be obtained from unloading then this necessity may be bypassed. A problem arises in the choice of the appropriate ϕ value to describe the unloading, and this is discussed further in a later section.

THEORY

Using a cylindrical coordinate system let the axial, radial and circumferential (hoop) stresses by denoted by σ_z, σ_r and σ_θ (compressive positive) and the corresponding strains by ϵ_z, ϵ_r and ϵ_θ. In the initial part of the analysis pore pressures will be assumed zero, so that total and effective stresses are equal; in the final discussion pore pressure will be denoted by u and effective stresses by the usual dash notation. The radial coordinate is r and radial displacement (assumed small compared to r) is ξ.

Plane strain conditions are assumed in the axial direction, so that $\epsilon_z = 0$, and the definitions of the other strains are:

$$\epsilon_r = -\frac{d\xi}{dr}$$

$$\epsilon_\theta = -\frac{\xi}{r}$$

The radial equilibrium equation for the stresses is written:

$$\frac{d\sigma_r}{dr} + \frac{\sigma_r - \sigma_\theta}{r} = 0$$

At the outer boundary ($r = \infty$) the boundary conditions $\sigma_r = \sigma_\theta = \sigma_{ho}$ (where σ_{ho} is the in situ horizontal stress) and $\xi = 0$ will be used. At the inner boundary the radius of the pressuremeter is denoted by a, the value of σ_r at a by ψ and the value of $\frac{\xi}{r}$ ($= -\epsilon_\theta$) at a by ϵ. Prior to cavity expansion $\xi = 0$ and $\sigma_r = \sigma_\theta = \sigma_{ho}$ at all r.

Loading

The soil is assumed to behave initially in an isotropic elastic manner. Under the conditions of plane strain in the axial direction and axial symmetry the result for the case of the outer boundary at infinity is well known at any radius as:

$$d\sigma_r = -2Gd\epsilon_\theta$$

i.e.

$$\sigma_r = \sigma_{ho} - 2G\epsilon_\theta$$

(Note that ϵ_θ is negative on loading). In particular at the pressuremeter:

$$d\psi = 2Gd\epsilon$$

$$\psi = \sigma_{ho} + 2G\epsilon$$

Note that the only elastic property which enters the analysis is the shear modulus G.

Additionally it can easily be shown that during the elastic phase $d\epsilon_r = -d\epsilon_\theta$ and $d\sigma_r = -d\sigma_\theta$. It follows that in the elastic region there is no volumetric strain and also no change in mean stress $\sigma = \frac{\sigma_r + \sigma_\theta}{2}$. It is useful before proceeding further to eliminate ξ between the definitions for the strain rates to obtain the strain compatability relation:

$$\frac{d\epsilon_\theta}{dr} + \frac{\epsilon_\theta - \epsilon_r}{r} = 0$$

The plastic behaviour of the soil is assumed to conform to the following conditions. The soil is assumed to behave as an elastic - plastic material in which the yield surface is given by the (cohesionless) Mohr-Coulomb condition:

$$\frac{\sigma_1}{\sigma_3} = \frac{(1 + \sin\phi)}{(1 - \sin\phi)} = \frac{1}{N} > 1$$

where the parameter N is introduced to simplify some of the subsequent mathematics. Thus on loading, assuming that the axial stress is the intermediate stress:

$$\frac{\sigma_\theta}{\sigma_r} = N$$

and the equilibrium equation may be re-written as:

$$\frac{d\sigma_r}{dr} + \frac{\sigma_r}{r}(1 - N) = 0$$

which has the solution

$$\sigma_r = Ar^{(N - 1)}$$

It follows that the stresses at two radii r_o and r_1 are related by:

$$\frac{\sigma_{ro}}{\sigma_{r1}} = \left[\frac{r_o}{r_1}\right]^{(N - 1)} \qquad ...(1)$$

and in particular:

$$\frac{\psi}{\sigma_{r1}} = \left[\frac{a}{r_1}\right]^{(N - 1)}$$

During the plastic behaviour it is assumed that the soil dilates with an angle of dilation ν:

$$\frac{d\epsilon_1}{d\epsilon_3} = - \frac{(1 - \sin \nu)}{(1 + \sin \nu)} = - n \geq -1$$

[Note that, for simplicity of the mathematics, the angle of dilation refers to the total strains not the conventionally defined plastic strains. In other words once plasticity occurs the elastic strains are ignored. It is possible to carry out all the following analysis accounting for elastic and plastic strains in the plastic region but the mathematics is more complex.]

Thus on loading, the strains in the plastic region are given by:

$$\frac{d\epsilon_r}{d\epsilon_\theta} = - n$$

so that:

$$\frac{(\epsilon_r - \epsilon_r^{ip})}{(\epsilon_\theta - \epsilon_\theta^{ip})} = - n \qquad ...(2)$$

where the superscript 'ip' refers to the strain causing initiation of plasticity for that particular soil element. The compatability equation becomes:

$$\frac{d\epsilon_\theta}{dr} + \frac{\epsilon_\theta}{r}(1 + n) = \epsilon_r^{ip} + n\,\epsilon_\theta^{ip} = f(r) \quad ...(3)$$

This may be integrated to give:

$$\epsilon_\theta = Br^{-(1+n)} + g(r)$$

It follows that the hoop strains at two radii are related by:

$$\frac{\epsilon_{\theta o} - g(r_o)}{\epsilon_{\theta 1} - g(r_1)} = \left[\frac{r_o}{r_1}\right]^{-(1+n)} \quad ...(4)$$

and in particular:

$$\frac{-\epsilon - g(a)}{\epsilon_{\theta 1} - g(r_1)} = \left[\frac{a}{r_1}\right]^{-(1+n)}$$

where g(r) is the particular integral for f(r). In particular when f(r) takes the form of the power expression ar^b then g(r) is equal to $\frac{ar^b}{(b + (1 + n))}$. For the special case b = 0 (i.e. f(r) = a) this expression is still true and $g(r) = \frac{a}{(1 + n)}$.

The expressions describing the plastic behaviour may now be combined to determine the relationship between ψ and ϵ during plasticity.

Since during elastic behaviour $d\sigma_r = -d\sigma_\theta$, yield of the soil at any radius occurs when:

$$\sigma_r = \sigma_{ho} + \sigma_{ho}\sin\phi$$

$$\sigma_\theta = \sigma_{ho} - \sigma_{ho}\sin\phi$$

Thus at the edge of the plastic zone $\sigma_r - \sigma_{ho} = \sigma_{ho}\sin\phi$ and $\epsilon_\theta = -\frac{\sigma_{ho}\sin\phi}{2G}$. The elastic portion of the loading curve in (ϵ, ψ) space is therefore from (0, σ_{ho}) to ($\frac{\sigma_{ho}\sin\phi}{2G}$, $\sigma_{ho} + \sigma_{ho}\sin\phi$). The pressuremeter strain at the initiation of plasticity will be referred to as ϵ^{ip} which is given by:

$$\epsilon^{ip} = \frac{\sigma_{ho} \sin\phi}{2G}$$

Note that the strain at any radius as plasticity is initiated at that radius is given by:

$$\epsilon_r^{ip} = \epsilon^{ip}$$
$$\epsilon_\theta^{ip} = -\epsilon^{ip}$$

Consider now the case when plastic deformation has extended to a radius r_1. The function f(r) in equation (3) is given by:

$$f(r) = \epsilon^{ip}(1 - n)$$

so that:

$$g(r) = \epsilon^{ip} \frac{(1 - n)}{(1 + n)} = \epsilon^{ip} \sin\nu$$

The relationship between strains, equation (4) now becomes:

$$\frac{-\epsilon - \epsilon^{ip}\sin\nu}{-\epsilon^{ip} - \epsilon^{ip}\sin\nu} = \left[\frac{a}{r_1}\right]^{-(1 + n)} \qquad ...(5)$$

and the relationship between stresses gives:

$$\frac{\psi}{\sigma_{ho} + \sigma_{ho}\sin\phi} = \left[\frac{a}{r_1}\right]^{(N - 1)} \qquad ...(6)$$

Eliminating r_1 between equations (5) and (6) and re-arranging gives:

$$\psi = \sigma_{ho}(1 + \sin\phi)\left[\frac{\frac{\epsilon}{\epsilon_{ip}} + \sin\nu}{1 + \sin\nu}\right]^{\left[\frac{1 - N}{1 + n}\right]} \qquad ...(7)$$

This result is exactly as obtained by Hughes, Wroth and Windle [1] but has been derived using a **slightly** different method here. The new method is introduced because it proves to be easier to use in the analysis of the unloading.

Figure 1 shows schematically the state of the soil at the end of loading. The soil between A and E has been loaded elastically along the line OFE in Figure 1(b) and then plastically along ECA. Points with the same letters in Figures 1(a) and 1(b) refer to the same soil element at the end of loading. Soil outside the radius E is still elastic.

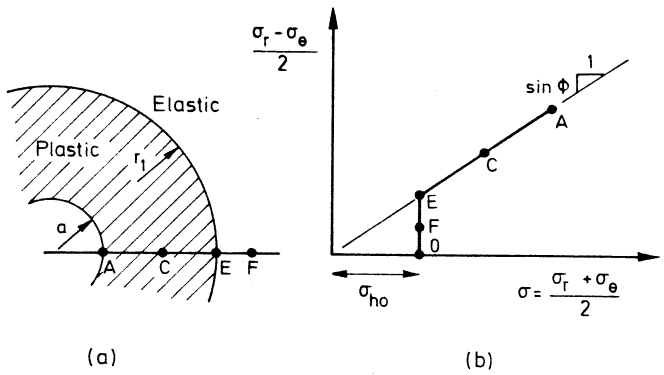

(a) (b)

FIG. 1--Stress state at the end of loading

Unloading

The unloading stage of the test begins by a purely elastic stage. This continues until the radial stress is reduced sufficiently so that plastic deformation in the opposite direction from the loading occurs. Note that at the end of loading at the pressuremeter surface:

$$\psi = \psi_1 = \sigma_r = \sigma + \sigma \sin \phi$$
$$\sigma_\theta = \sigma - \sigma \sin \phi$$

during the elastic unloading there is no change in σ, so that when reverse plasticity is initiated:

$$\psi = \sigma_r = \sigma - \sigma \sin \phi$$
$$\sigma_\theta = \sigma + \sigma \sin \phi$$

so that $\psi = \frac{\psi_1}{N}$.

If ϵ_1 is the pressuremeter strain at ψ_1 the elastic unloading is therefore from (ϵ_1, ψ_1) to $(\epsilon_1 - \frac{\psi_1(1 - \frac{1}{N})}{2G}, \frac{\psi_1}{N})$.

Reverse plasticity then occurs in a region which gradually spreads out from the pressuremeter. In this region the stresses are related by:

$$\frac{\sigma_\theta}{\sigma_r} = \frac{1}{N}$$

so that the analysis of the stresses is exactly as before except with N replaced by $\frac{1}{N}$. In particular one may write:

$$\frac{\psi}{\sigma_{r2}} = \left[\frac{a}{r_2}\right]^{(\frac{1}{N} - 1)} \qquad \ldots(8)$$

During the reverse plasticity the strain rates are related by:

$$\frac{d\epsilon_r}{d\epsilon_\theta} = -\frac{1}{n}$$

so that the analysis of the strains is also as before, except that n is replaced by $\frac{1}{n}$. In particular the result is obtained:

$$\frac{-\epsilon - g^*(a)}{-\epsilon_{\theta 2} - g^*(r_2)} = \left[\frac{a}{r_2}\right]^{-(1+\frac{1}{n})} \quad \ldots(9)$$

Where $g^*(r)$ is the particular integral for $f^*(r)$ where:

$$f^*(r) = \epsilon_r^{irp} + \frac{1}{n}\epsilon_\theta^{irp}$$

and the superfix 'irp' indicates the strain at the initiation of reverse plasticity.

If $f^*(r)$ is of the form of the power expression ar^b then $g^*(r)$ is equal to $\frac{ar^b}{(b+(1+\frac{1}{n}))}$.

The analysis may now proceed on exactly similar lines to the analysis of the loading, except that the determination of the strains on the initiation of unloading is slightly more complex.

The radial stress at radius r in the plastic zone at the end of loading is derived from equation (1).

$$\sigma_r = \sigma_{ho}(1+\sin\phi)\left[\frac{r}{r_1}\right]^{(N-1)}$$

and the hoop strain is given by comparison with equation (4) as:

$$\epsilon_\theta = \epsilon^{ip}\left[\sin\nu - (1+\sin\nu)\left[\frac{r}{r_1}\right]^{-(1+n)}\right]$$

Making use of equation (2) one may derive:

$$\epsilon_r = \epsilon^{ip}\left[\sin\nu + (1-\sin\nu)\left[\frac{r}{r_1}\right]^{-(1+n)}\right]$$

During the elastic unloading the mean stress σ remains constant, so that the value of σ_r when reverse plasticity occurs at r is given by:

$$\sigma_r = \sigma_{ho}\,(1 - \sin\phi)\left[\frac{r}{r_1}\right]^{(N-1)}$$

and that the associated increment of the hoop and radial strains result in expressions for the strains at the beginning of reverse plasticity:

$$\epsilon_r^{irp} = \epsilon^{ip}\left[\sin\nu + (1 - \sin\nu)\left[\frac{r}{r_1}\right]^{-(1+n)} - 2\left[\frac{r}{r_1}\right]^{(N-1)}\right]$$

$$\epsilon_\theta^{irp} = \epsilon^{ip}\left[\sin\nu - (1 + \sin\nu)\left[\frac{r}{r_1}\right]^{-(1+n)} + 2\left[\frac{r}{r_1}\right]^{(N-1)}\right]$$

So that $f^*(r)$ is given by:

$$f^*(r) = \epsilon^{ip}(1 - n)\left[1 - 2\left[\frac{r}{r_1}\right]^{-(1+n)} + 2\left[\frac{r}{r_1}\right]^{(N-1)}\right]$$

and $f^*(r)$ has the particular integral:

$$g^*(r) = \epsilon^{ip}\left[\sin\nu - \frac{2}{(1+n)}\left[\frac{r}{r_1}\right]^{-(1+n)} + \frac{2(1-N)}{(1+nN)}\left[\frac{r}{r_1}\right]^{(N-1)}\right]$$

Note that at $r = a$ the expression simplifies to:

$$g^*(a) = -\epsilon_1 + \frac{\psi_1(1-n)(1-N)}{2G(1+nN)}$$

If, after plasticity on loading to a radius of r_1, reverse plasticity occurs to a radius of r_2 ($a < r_2 < r_1$) then the expression for the stress, equation (8) gives:

$$\frac{\psi}{\sigma_{ho}(1+\sin\phi)\left[\frac{r_2}{r_1}\right]^{(N-1)}} = \left[\frac{a}{r_2}\right]^{(\frac{1}{N}-1)}$$

and the expression for the strain, equation (9), gives:

$$\frac{\left[-\epsilon - \epsilon_1 - \frac{\psi_1(1-n)(1-N)}{2G(1+nN)}\right]}{\epsilon^{ip}\left[-(1+\sin\nu)\left[\frac{r}{r_1}\right]^{-(1+n)} + 2\left[\frac{r}{r_1}\right]^{(N-1)} + \frac{2}{(1+n)}\left[\frac{r}{r_1}\right]^{-(1+n)} - \frac{2(1-N)}{(1+nN)}\left[\frac{r}{r_1}\right]^{(N-1)}\right]}$$

$$= \left[\frac{a}{r_2}\right]^{-(1+\frac{1}{n})}$$

This may be considerably simplified to:

$$2G(1 + nN)(\epsilon_1 - \epsilon) - \psi_1(1 - n)(1 - N) = \psi_1 n(1 - N^2)\left[\frac{r_2}{a}\right]^{(N + \frac{1}{n})}$$

Finally r_2 may be eliminated to give:

$$\psi = n\psi_1\left[\frac{\frac{2G(1 + nN)(\epsilon_1 - \epsilon)}{(1 - N)\psi_1} - (1 - n)}{n(1 + N)}\right]^{\left[\frac{N - \frac{1}{N}}{N + \frac{1}{n}}\right]} \quad \ldots(10)$$

which is the relationship between ψ and ϵ on plastic unloading. Figure 2 shows diagrammatically the state of the soil after plastic unloading to a radius of r_2. Points A and B have initially been loaded elastically, then plastically to A_1, and B_1. They have then unloaded elastically at constant σ and finally unloaded plastically to A and B. Points C and D have been through a similar history, except that C has just reached the beginning of plastic unloading and D has not yet reached it. Points E and F have been loaded and unloaded elastically.

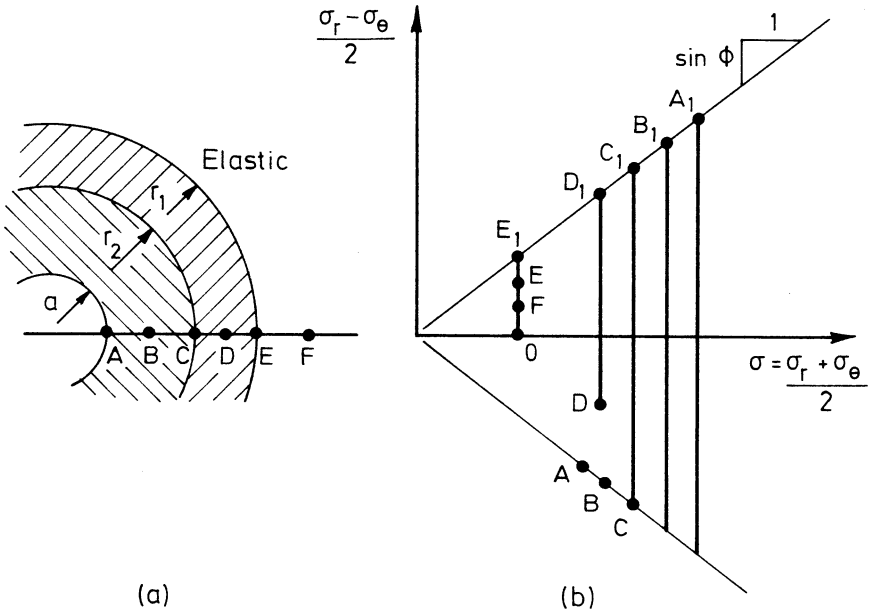

FIG. 2—Stress state after unloading

The above solution applies until r_2 becomes equal to r_1, at which stage ϵ is given by ϵ_2 where:

$$\epsilon_2 = \epsilon_1 - \frac{\psi_1(1 - n)(1 - N)}{2G(1 + nN)} - \frac{\epsilon^{ip}{}_{2n(1 + N)}}{1 + nN}\left[\frac{\psi_1}{\sigma_{ho} + \sigma_{ho}\sin\phi}\right]^{\left[\frac{1 + \frac{1}{n}}{1 - N}\right]}$$

Although it has not been possible to show the following result in general, it has been shown for a wide variety of parameter values that ϵ_2 is negative. It follows that r_2 remains smaller than r_1 unless the pressuremeter diameter can be reduced to less than the original installation diameter. The solution for $r_2 > r_1$ is not therefore relevant to existing pressuremeter designs.

THE STRESS-DILATANCY RELATIONSHIP

The two parameters ϕ and ν are not independent, since for a given sand it is known that as the density increases both the angle of dilation and the angle of friction increase together. The relationship between ϕ and ν is conveniently expressed by using Rowe's stress-dilatancy relation [3], which is well known to fit the behaviour of many sands well. The relation may be expressed as:

$$\left[\frac{1 + \sin\phi}{1 - \sin\phi}\right] = \left[\frac{1 + \sin\phi_{cv}}{1 - \sin\phi_{cv}}\right]\left[\frac{1 + \sin\nu}{1 - \sin\nu}\right]$$

where ϕ_{cv} is the angle of friction at constant volume. The value of ϕ_{cv} may be determined from tests on disturbed samples, so that by making an independent measurement of ϕ_{cv} the stress dilatancy relation can be introduced and only one of the parameters ϕ and ν in the pressuremeter analysis needs to be treated as an unknown.

PORE PRESSURES

All the above analysis assumes that the pore pressures are zero. In practice the pore pressure in a sand will not be zero, but if the sand is highly permeable it may be assumed that the pore pressure throughout the test remains at the initial pore pressure u_o (which will often be equal to the hydrostatic pore pressure). In this case the analysis is unaltered and all the above stresses should be interpreted as effective stresses, to obtain total stresses u_o must be added to the values of each of the stresses in the above analysis. In the remainder of the paper the pore pressure will be taken as u_o and the stresses will be denoted as effective stresses by a dash notation e.g. σ'_{ho}. Since on unloading the value of the effective pressuremeter pressure ψ' rapidly falls to a very small value, the total pressure ψ on unloading may be used as an estimate of u_o.

ANALYSIS OF FIELD DATA

The analysis described above has been used to interpret data obtained from self-boring pressuremeter (SBP) tests carried out as part of an investigation of the soil types and properties at the site of the Shotton Paper Mill, North Wales, U.K. The site was the former British Steel Shotton Works. It is level with uniformly graded fine to coarse sand extending from ground level to at least 20m depth. The ground water level is at a depth of 3.8m and the pore pressure profile is hydrostatic.

The instrument used, similar to that described by Windle and Wroth [4], was 83.4mm in diameter and 1050mm long, with the expanding section being 500mm long. The importance and uniqueness of the SBP is that, using correct drilling techniques, it is possible to insert it into the ground causing minimal disturbance to the surrounding soil. Although it is difficult to drill the SBP into sand, improved techniques mean it is now possible to insert the SBP into the ground causing minimal disturbance (Clarke and Wroth, [5]).

Figure 3 shows a typical test carried out at 5.8m below ground level. The total applied membrane pressure ψ corrected for the membrane stiffness is plotted against the cavity strain ϵ. The total lateral stress σ_{ho} is taken directly from the curve and is equal to $96kN/m^2$ giving a value of 0.90 for the coefficient of earth pressure at rest K_o. The shear modulus of $52MN/m^2$ is taken from the unload/reload loop. The loading portion of the curve was analysed using the method of Hughes et al. [1] to give a value of the angle of friction of 37°.

The field data were recorded with the aid of a microcomputer. An optimisation routine was written for a microcomputer to analyse the data using the above analysis. The analysis involves five soil parameters: pore pressure u_o, total lateral stress σ_{ho}, shear modulus G, angle of friction ϕ, and angle of dilation ν. The pore pressure profile at this site was known, and the total lateral stress taken directly from the test curve. Thus there are only three variables to be optimised, and two of those are related by Rowe's stress dilatency law. It may be expected at many sites that the ϕ_{cv} value will be known, but unfortunately no data were available from this site.

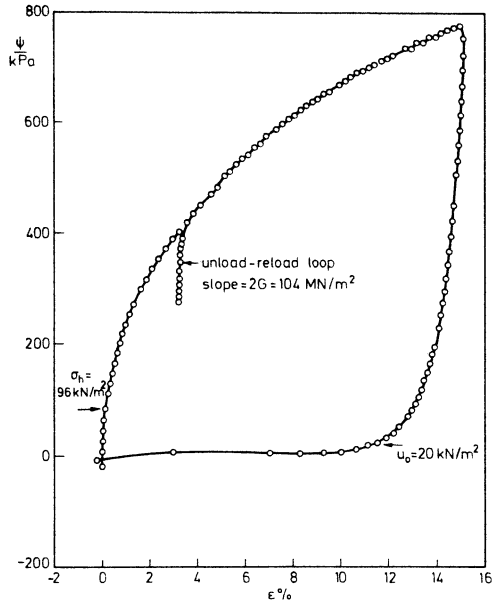

FIG. 3--Pressuremeter curve for test at 5.8m

In the analysis it is assumed that G is constant both for loading and unloading. There is evidence that G varies throughout the test (Clarke and Wroth [3]), and Figures 4 and 5 show the G values taken from the unload/reload loops for the tests at this site. Fig. 4 shows the values plotted against depth and Fig. 5 shows them plotted against the mean effective stress at the pressuremeter surface at which they were measured. There is considerably less scatter in Fig. 5. However, for the purposes of this analysis it will be assumed G is constant over each of four sections of the test, initial elastic loading (G_{EL}), plastic loading (G_{PL}), initial elastic unloading (G_{EU}) and plastic unloading (G_{PU}). Separate moduli values will be reported for each of these sections.

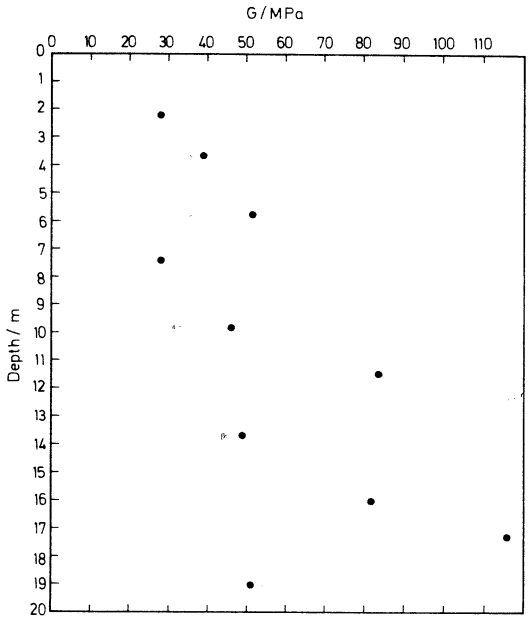

FIG. 4--Unload-reload shear moduli v. Depth

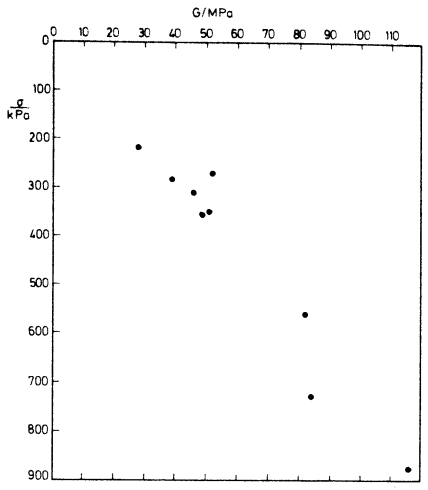

FIG. 5--Unload-reload shear moduli v. mean stress at pressuremeter

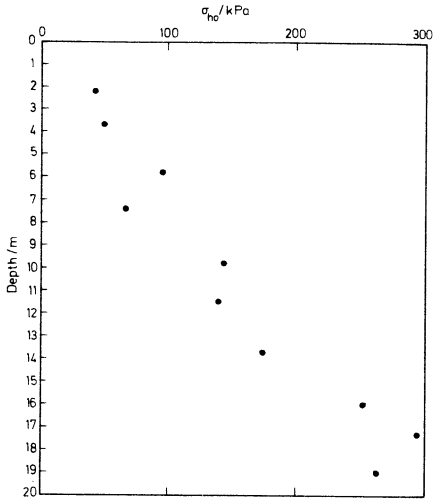

FIG. 6--Variation of total lateral stress σ_{ho} with depth

Figure 6 shows the observed variation in total lateral stress with depth. Using a unit weight of 18kN/m^3 and the known pore pressure profile the variation of K_o with depth can be calculated. The implication is that the sand is overconsolidated, with the degree of overconsolidation varying with depth. Therefore the sand is likely to exhibit a peak ϕ on loading. The value of ϕ on unloading (ϕ_U) will depend on the amount the membrane has expanded before unloading. If the membrane expansion is sufficient for the sand to reach critical state, so that the angle of friction is that at constant volume ϕ_{cv}, then on unloading the appropriate ϕ_U is likely to equal ϕ_{cv}. This represents a lower bound on the ϕ_U value. The upper bound may be appropriate if the membrane has just expanded sufficiently to bring the sand to the peak deviator stress, then ϕ_U is likely to equal ϕ_L (the loading ϕ). Thus three cases for analysis can be identified.

(a) $\phi_U = \phi_L$

(b) $\phi_U = \phi_{cv}$

(c) $\phi_L \neq \phi_U \neq \phi_{cv}$

For all cases it is assumed that ϕ_{cv} is constant and Rowe's stress dilatancy is assumed to apply. An outline of the program for the microcomputer used for analysing the test is now described:

(a) input u_o, σ_{ho}, ϕ_{cv}

(b) label the loading portion of the curve as that from σ_{ho} to the maximum applied stress

(c) label the unloading portion of the curve as that from the maximum applied stress to u_o

(d) using an initial estimate $\phi_L = \phi_{cv}$ determine a yield point in compression

(e) optimize the plastic loading expression to give values of G_{PL} and ϕ_L (Eq. 7)

(f) repeat step (e) with the new yield point until the optimum values of G_{PL} and ϕ_L are acheived

(g) calculate G_{EL} from the loading data from before the yield point

(h) using an initial estimate of $\phi_U = \phi_{cv}$ determine a yield point in extension

(i) optimize the plastic unloading expression to give values of G_{PU} and ϕ_U (Eq. 10) (this stage is simplified if $\phi_U = \phi_{cv}$ or $\phi_U = \phi_L$ is used)

(j) repeat step (i) with a new yield point until the optimum values of G_{PU} and ϕ_U are achieved

(h) calculate G_{EU} from the unloading section before yield

The optimisation routine was carried out by calculating ψ for the measured values of cavity strain and comparing them with the measured values of ψ. Table 1 gives the results for test 3 at 5.8m depth using each of the three cases above. Figure 7 shows a comparison between the optimum curve and the field curve for Case (b), $\phi_U = \phi_{cv}$.

TABLE 1--Test at 5.8m depth interpreted using different assumptions

Case	Loading			Unloading		
	G_{EL}	G_{PL}	ϕ_L	G_{EU}	G_{PU}	ϕ_U
(a) $\phi_U = \phi_L$	9050	4300	60°	20940	21250	60°
(b) $\phi_U = \phi_{cv}$	9060	10310	40°	37830	35050	29°
(c) $\phi_U \neq \phi_L \neq \phi_{cv}$	9050	10040	43°	37830	35050	29°

The following points can be noted:

(a) The Case (a) assumption $\phi_U = \phi_L$ results in very high ϕ values and implies that $G_{EL} > G_{PL}$, which is not consistent with the notion that G increases with effective stress. This case therefore seems unrealistic.

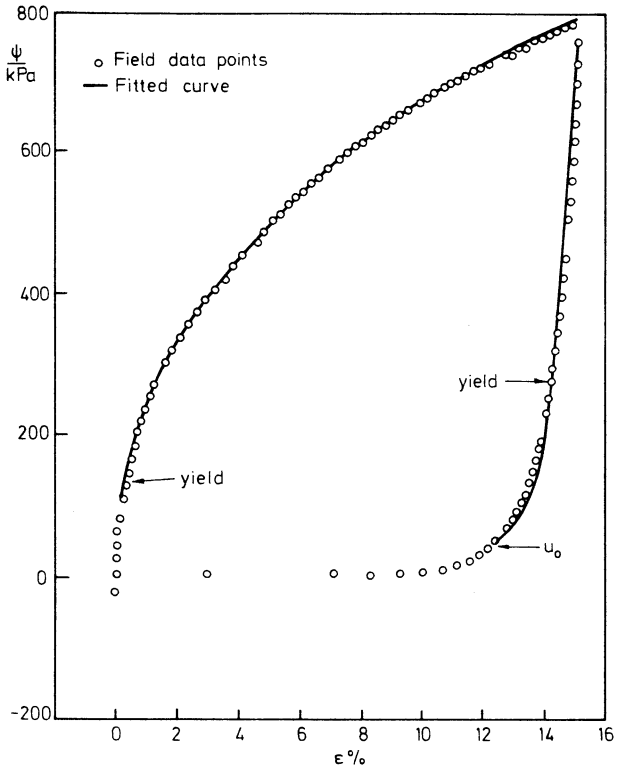

FIG. 7--Measured and fitted pressuremeter curve for test at 5.8m

(b) Case (c), $\phi_L \neq \phi_U \neq \phi_{cv}$ results in moduli which are consistent with the notion that G increases with effective stress. However, for this case $\phi_{cv} = 35°$, which is inconsistent with the analysis which requires that $\phi_U \geq \phi_{cv}$.

(c) Comparison between Cases (b) and (c) shows that ϕ_U is insensitive to the value of ϕ_{cv}. This was found to be the case in the majority of the tests. This comparison also shows that a decrease in ϕ_{cv} of

6° implies a reduction in ϕ_L of 3°. This is consistent with the analysis of Hughes et al. [1].

(d) Small differences in G are a result of the numerical calculations.

(f) There are many data points for the plastic loading of the soil, whereas for the plastic unloading there are few.

As ϕ_U is insensitive to the value of ϕ_{cv}; ϕ_U is unlikely to be equal to ϕ_L and using $\phi_U = \phi_{cv}$ gives a conservative value of ϕ_L, it would seem reasonable that the test should be analysed assuming $\phi_U = \phi_{cv}$. This has the advantage that further laboratory data are not required. These observations were found to be similar in all the tests analysed.

Table 2 gives the result of the interpretation of all the tests assuming $\phi_U = \phi_{cv}$. There is scatter in the results. This is not inconsistent with field and laboratory measurements on other soils and reflects the non-homogeneity of sands. Further inspection of the total stress measurements indicate that the geological history of the site may be complex with the sand being deposited in layers at different times and possibly from different sources.

TABLE 2--Results of tests assuming $\phi_U = \phi_{cv}$

Depth, m	σ_{ho}	u_o	G_{EL}	G_{PL}	ϕ_L	G_{EU}	G_{PU}	$\phi_U = \phi_{cv}$
2.2	43	0	3650	5040	48°	37480	40310	22°
5.8	96	20	9060	10310	40°	37830	35050	29°
9.8	130	59	5780	6690	49°	28820	29130	34°
13.7	174	97	4700	4950	47°	44010	42950	24°
17.3	222	132	-	27400	47°	96010	88080	26°
19.0	262	149	2930	3090	49°	52730	50530	23°

The effect of varying σ_{ho} was also investigated. A change of 25% induced a change of approx 1° in ϕ_L. If the correct drilling techniques are used is should be possible to determine σ_{ho} accurately. However, in many sand tests there is some disturbance. No investigation has been undertaken of the effects of analysing disturbed tests.

Inspection of Fig. 4 shows that the value of modulus derived from the unload/reload loop is greater than G_{EU}, but the effective stress is less. The value of G varies not only with the effective stress at which it is measured but also the stress range over which it is measured.The stress range for the unload/reload loop is less than the difference between the maximum applied stress and the yield point in extension therefore the results may not be inconsistent.

Unlike the case at this site, the pore pressure is often unknown. Wroth [4] describes how the pore pressure can be estimated from the point on unloading at which the membrane begins to contract rapidly due to the pressure of the water balancing the applied pressure. Inspection

of Fig. 8 shows the pore pressure estimated by this method is up to 25% less than that derived from the hydrostatic profile. The test at 5.8m was analysed for different values of pore pressure and it was found that a 25% change in pore pressure changed ϕ_L by approx 1°. This change is small compared to all the other unknowns and assumptions, and therefore the estimated value could be used.

ACKNOWLEDGEMENT

The authors are grateful to the Shotton Paper Company Ltd. and Laing-Loy Management Contracting Ltd. for permission to use the field data presented in this paper.

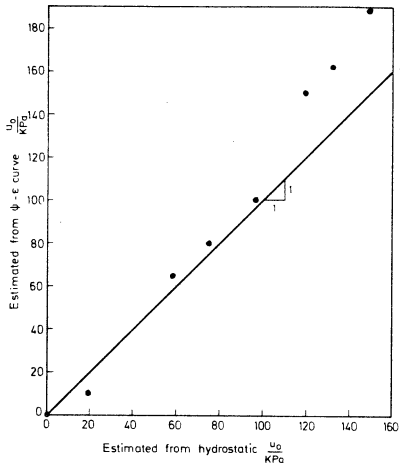

FIG. 8--Pore pressures estimated from hydrostatic profile and pressuremeter tests

REFERENCES

[1] Hughes, C.M.O., Wroth, C.P., and Windle, D.J., "Pressuremeter Tests in Sands", Geotechnique, Vol. 27, No. 4, pp. 455-478, Dec. 1977

[2] Gibson, R.E. and Anderson, W.F., "In Situ Measurement of Soil Properties with the Pressuremeter", Civ. Eng. Pub. Works Review, Vol. 56, No. 658, pp. 615-618, May 1961

[3] Rowe, P.W., "The Stress-Dilatancy Relation for Static Equilibrium of an Assembly of Particles in Contact", Proc. Roy. Soc., Vol. 269A, pp. 500-527, 1971

[4] Windle, D.J. and Wroth, C.P., "The Use of the Self-Boring Pressuremeter to Determine the Undrained Properties of Clays", Ground Engineering, Vol. 10, No. 1, pp.37-46, Jan. 1977

[5] Clarke, B.G. and Wroth, C.P., Discussion on "Effect of Disturbance on Parameters Derived from Self-Boring Pressuremeter Tests in Sand", Geotechnique, Vol. 35, No. 2, pp. 219-222, June 1985

[6] Wroth, C.P., "The Interpretation of In Situ Soil Tests", Geotechnique, Vol. 24, No. 4, pp. 447-492, Dec. 1984